Electronic Supplementary Material (ESI) for Chemical Science.

SUPPORTING INFORMATION

Destabilized reporters for background-subtracted, chemically-gated, and multiplexed deep-tissue imaging

Jason Yun[1#], Yimeng Huang[1#], Austin D.C. Miller[2], Brandon L. Chang[3], Logan Baldini[4], Kaamini M. Dhanabalan[4], Eugene Li[4], Honghao Li[1], Arnab Mukherjee[*1,2,4]

Affiliations:

[1]Department of Chemistry, University of California, Santa Barbara, CA 93106, USA

[2]Biomolecular Science and Engineering Graduate Program, University of California, Santa Barbara, CA 93106, USA

[3]Department of Molecular, Cell, and Developmental Biology, University of California, Santa Barbara, CA 93106, USA

[4]Department of Chemical Engineering, University of California, Santa Barbara, CA 93106, USA

[#] denotes equal contribution

*Correspondence should be addressed to AM (arnabm@ucsb.edu)

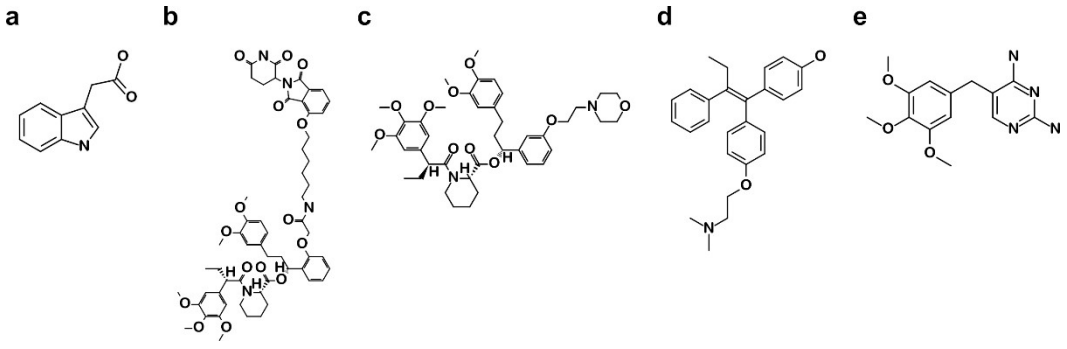

Supplementary figure 1. Chemical structures of the ligands tested for Aqp1 modulation. **(a)** indole-3-acetic acid, an auxin family hormone **(b)** dTAG-13, TAG-13, a heterobifunctional degrader that consists of an FKBP12^{F36V} targeting synthetic ligand (known as AP1687) linked to a thalidomide moiety, which recruits the cereblon E3 ubiquitin ligase **(c)** shield-1, a morpholine-containing derivative of the FKBP12^{F36V}-directed synthetic ligand, **(d)** 4-hydroxytamoxifen, and **(e)** trimethoprim. Indole-3-acetic acid and dTAG-13 are capable of inducing the degradation of protein targets that have been fused to degradation tags derived from IAA17 and FKBP12^{F36V}, respectively. On the other hand, 4-hydroxytamoxifen and trimethoprim are capable of stabilizing protein targets that have been fused to destabilizing domains (DDs) derived from the estrogen receptor ligand-binding domain and *E. coli* dihydrofolate reductase (DHFR). Additionally, shield-1 can either induce the degradation of proteins that are fused to a modified FKBP12^{F36V} domain comprising a 19-amino acid cryptic degron or stabilize proteins that are fused to a DD based on FKBP12$^{F36V/L106P}$ double mutant. Chemical structures were generated using PubChem Sketcher v2.4.

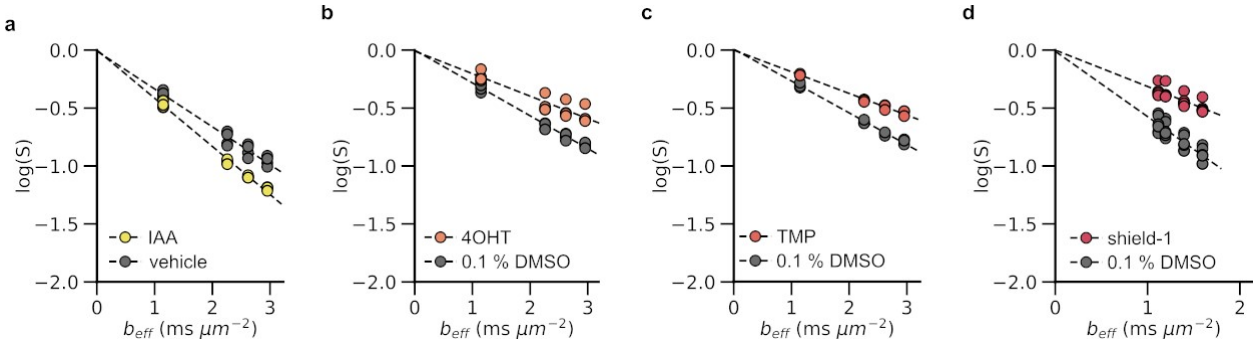

Supplementary figure 2. Effect of ligand-dependent DDs on Aqp1 diffusivity. Representative plots depicting the decrease in diffusion-weighted signal intensity as a function of the effective b-value in CHO cells engineered to express DDs based on: **(a)** truncated 68-amino acid form of the plant protein, IAA17 **(b)** estrogen receptor ligand-binding domain **(c)** *E. coli* dihydrofolate reductase **(d)** mammalian FKBP12$^{F36V/L106P}$. Diffusion-weighted measurements were acquired in both the absence and presence of treatment with the respective degradation-inducing ligand: indole-3-acetic acid (IAA) or stabilizing ligands: 4-hydroxytamoxifen (4HT), trimethoprim (TMP), and shield-1.

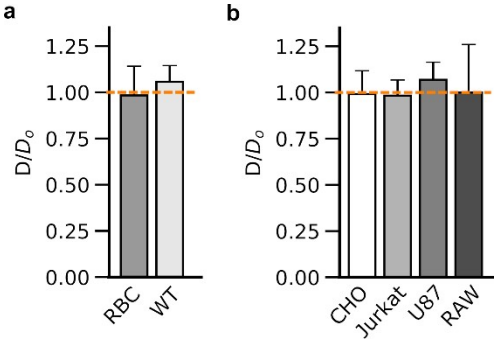

Supplementary figure 3: Specificity of shield-1 modulation. Fold-change in diffusivities (D/D_o) of **(a)** red blood cells and native CHO cells **(b)** cells engineered to express DD-free Aqp1 and treated with shield-1 (1 μM, 24-hours). Orange dashed line indicates no change relative to vehicle-treated controls. Error-bars represent the standard deviation (n = 4). Unpaired, 2-sided t-test revealed no significant differences in diffusivities between untreated cells and cells treated with 1 μM shield-1 for 24-hours ($P > 0.05$).

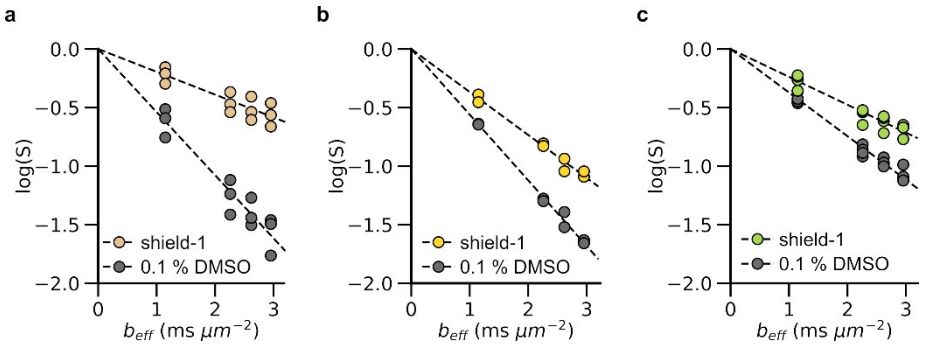

Supplementary figure 4. Biochemical modulation of Aqp1-FKBP12-DD in various cell lines. Representative plot showing the decrease in diffusion-weighted signal intensity as a function of the effective b-value in **(a)** Jurkat **(b)** U87 and **(c)** RAW cells engineered to express Aqp1-FKBP12-DD. Diffusion-weighted measurements were acquired in both the absence and presence of 24-hour treatment with 1 μM shield-1.

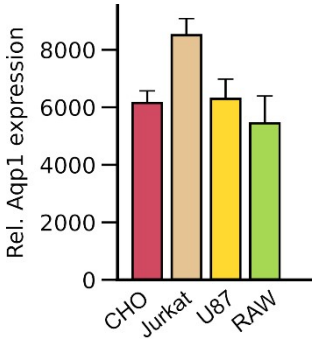

Supplementary figure 5. Expression of the Aqp1-FKBP12-DD transgene. Aqp1-FKBP12-DD expression was assayed by qRT-PCR using a forward primer that binds to the FLAG epitope sequence incorporated at the N-terminus of Aqp1. Actin was used as the housekeeping gene and relative Aqp1 expression was quantified using the $2^{-\Delta\Delta C_q}$ method. Error bars represent the standard deviation. One-way ANOVA followed by Tukey's HSD test revealed no significant differences in gene expression among the four cell types (n = 3, P > 0.05).

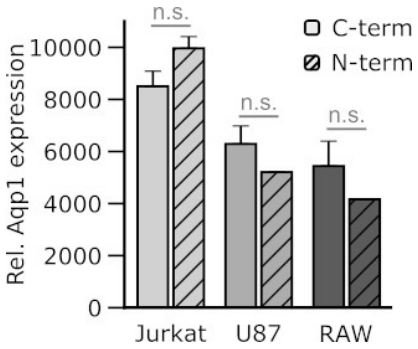

Supplementary figure 6. **Expression of Aqp1 harboring FKBP12-DD**. The expression of the FKBP12-DD-Aqp1 and Aqp1-FKBP12-DD transgenes was assayed by qRT-PCR using primers that bind to the FLAG epitope incorporated respectively at the C or N-terminus of Aqp1. Actin was used as the housekeeping gene and relative Aqp1 expression was quantified using the $2^{-\Delta\Delta C_q}$ method. Error bars represent the standard deviation. Unpaired, 2-sided t-test revealed no significant (n.s.) differences in transgene expression between cells expressing Aqp1 harboring either N or C-terminal fusions of FKBP12-DD ($P > 0.05$).

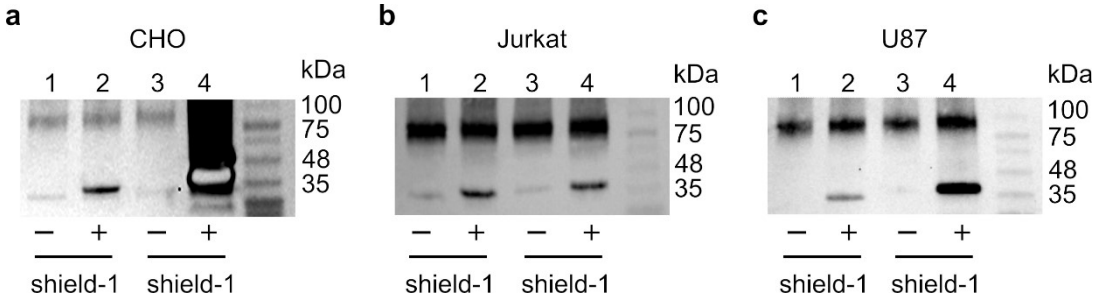

Supplementary figure 7. **Western blotting to detect Aqp1-FKBP12-DD expression**. Lysates were prepared from cells stably transduced to express Aqp1 harboring FKBP12-DD at either the C or N-terminus. Aqp1 expression was probed by immunostaining using an anti-FLAG antibody in **(a)** CHO **(b)** Jurkat and **(c)** U87 cells. Lanes 1 & 2 contain membrane fractions from cells expressing Aqp1 harboring FKBP12-DD at the C-terminus. Lanes 3 & 4 contain membrane extracts from cells expressing Aqp1 harboring FKBP12-DD at the N-terminus. The Na^+/K^+-ATPase pump (100 kDa) served as a loading control. The detection of FKBP12-DD-Aqp1 in

membrane extracts prepared from CHO cells proved to be challenging, as immunoblotting consistently led to the appearance of smeared bands.

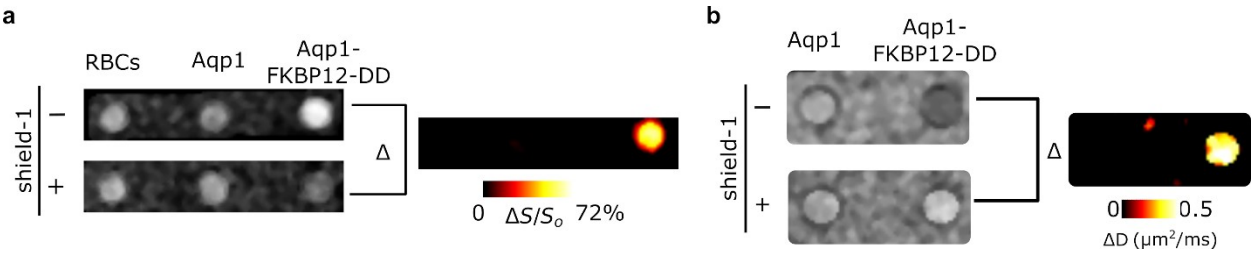

Supplementary figure 8. Differential imaging through shield-1 modulation. **(a)** Images of red blood cells and CHO cells expressing DD-free Aqp1 and Aqp1-FKBP12-DD that have undergone background subtraction. The difference image was produced by subtracting voxel-wise diffusion-weighted datasets acquired with and without shield-1 incubation, denoising the resulting image using a median filter, and displaying it as a pseudo colored "hotspot." **(b)** Diffusion maps of CHO cells expressing DD-free Aqp1 and Aqp1-FKBP12-DD that have undergone background subtraction. The difference map was produced by subtracting voxel-wise diffusivity values measured with and without shield-1 incubation, denoising the resulting image using a median filter, and displaying it in pseudo color.

a

shield-1	T_x	Output
0	0	0
1	0	0
0	1	0
1	1	1

b

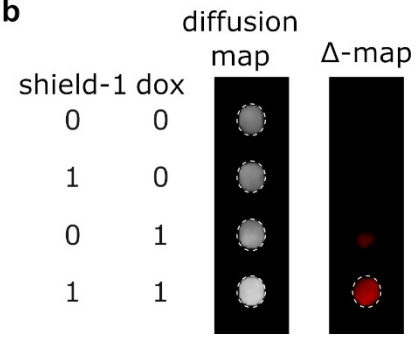

Supplementary figure 9. Biochemically-gated imaging of transcriptional activity. **(a)** Truth table for shield-1 gated imaging of promoter activity using Aqp1-FKBP12-DD. T_X represents the transcriptional activity induced by doxycycline (dox). **(b)** Difference map showing shield-1 gated imaging of promoter activity. The difference map was obtained through voxel-wise subtraction of

diffusivity values acquired in the presence of shield-1, doxycycline, or both from the diffusivity values measured in their absence. The resulting dataset was subsequently denoised using a median filter and presented as a pseudo-colored "hotspot."

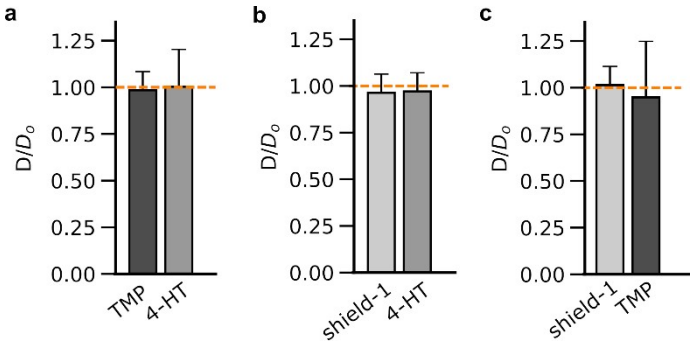

Supplementary figure 10: Aqp1-DDs are mutually orthogonal. Fold-change in the diffusion coefficients of **(a)** Aqp1-FKBP12-DD **(b)** Aqp1-DHFR-DD, and **(c)** Aqp1-ER-DD following treatment with respective non-cognate ligands, including trimethoprim (TMP) or 4-hydroxytamoxifen (4HT), and shield-1. Orange dashed lines indicate no change relative to vehicle-treated controls, *viz*. $D/D_o = 1$. Unpaired, 2-sided t-test revealed no significant differences in diffusivities between untreated and ligand-treated cells ($P > 0.05$).

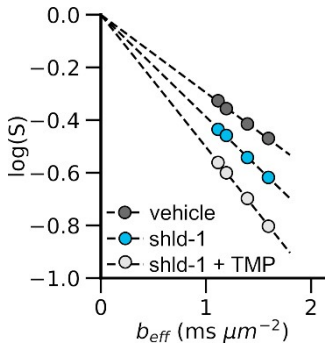

Supplementary figure 11. Biochemical modulation of Aqp1-DDs in mixed-cells. Representative plot showing the decrease in diffusion-weighted signal intensity as a function of the effective b-value in a 1:1 mixture of CHO cell labeled with Aqp1-FKBP12-DD and Aqp1-DHFR-DD. Diffusion-weighted measurements were acquired in both the absence of any ligand and following 24-hour treatment with shield-1 and both shield-1 + trimethoprim.

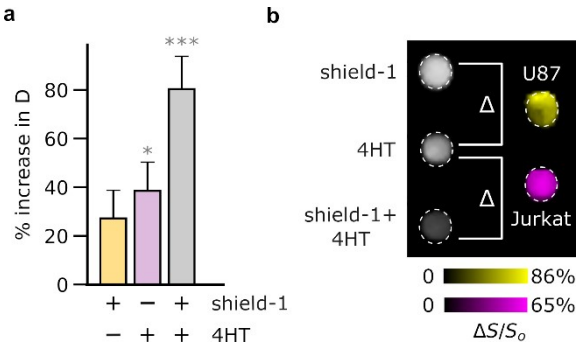

Supplementary figure 12: Biochemical unmixing of Aqp1-DDs for multiplex imaging. (a) Ligand-dependent increase in the diffusivity of a mixed population comprising U87 and Jurkat cells transduced respectively with Aqp1-FKBP12-DD and Aqp1-ER-DD transgenic reporters. Ligand addition permits the modulation of diffusivity in a stepwise manner by stabilizing one or both Aqp1-DD constructs. **(b)** The components of the mixed cell population were resolved through difference imaging. Subtraction of diffusion-weighted images of untreated cells from images acquired after treatment with shield-1 reveals the U87 population. Subtraction of diffusion-weighted images of shield-1 treated cells from those obtained after treatment with both shield-1 + 4-hydroxytamoxifen (4HT) revealed the Jurkat population. The images were denoised by median filtering and pseudo-colored to distinguish the two sub-populations. Error bars represent standard deviation (n = 6). P-values were computed using one-way ANOVA followed by Tukey's HSD test. * denotes $P < 0.05$, *** denotes $P < 0.001$

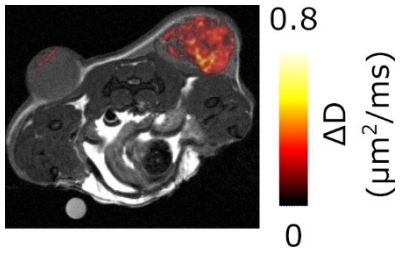

Supplementary figure 13. In vivo imaging using background subtraction. Background subtracted diffusion maps of transgenic tumors engineered to express Aqp1-FKBP12-DD or DD-free Aqp1. The difference map was generated by subtracting voxel-wise tumor diffusivity datasets

acquired before and after intraperitoneal injection of shield-1 (10 mg/kg). This difference map was then overlaid on an anatomical image to provide spatial context.

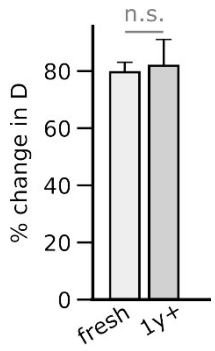

Supplementary figure 14. Longevity of reporter transgene activity. Shield-1-driven changes in the diffusivity of CHO cells transduced to express Aqp1-FKBP12-DD were acquired within 1-2 weeks of transduction and more than a year after initial transduction. Error bars denote standard deviation (*n* = 4-6). Unpaired, 2-sided t-test revealed no significant differences in shield-1 triggered diffusivity changes between the two cell batches ($P > 0.05$).

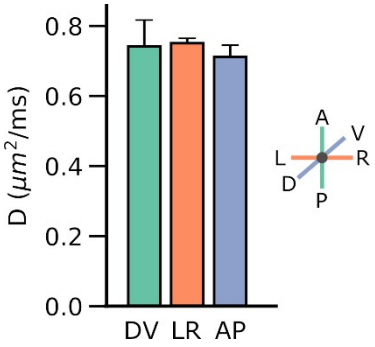

Supplementary figure 15. Effect of varying diffusion-weighting direction on Aqp1-driven diffusivity. Diffusivities of CHO cells engineered to express Aqp1 acquired in the 3 primary axes of our vertical-bore MRI: dorsal-ventral (DV), left-right (LR), and anterior-posterior (AP). Axial slices of cell pellets are acquired along the AP axis. One-way ANOVA followed by Tukey's HSD test revealed no significant differences in diffusivities between the three cardinal directions (*n* = 3, $P > 0.05$).

Table S1. Plasmids engineered and used in this study.

Plasmid	Main constructs encoded	Notes
pJY22	Flag-Aqp1-IRES-EGFP	Constitutive expression of degron-free Aqp1 from the EF1α promoter
pJY02	Flag-Aqp1-IAA17-IRES-EGFP	Expresses Aqp1 tagged to the auxin-inducible degron (AID) based on full-length IAA17 (228 amino acids)
pJY09	OsTIR1-IRES-mCherry	Constitutive expression of OsTIR1, an auxin receptor F-box protein that is needed to activate AID by recruiting E3 ubiquitin ligase
pJY19	Flag-Aqp1-IAA17^{trunc}-IRES-EGFP	Expresses Aqp1 tagged to truncated AID based on a 68-amino acid segment of IAA17
pJY18	AtFB2-IRES-mCherry	Constitutive expression of AtFB2, an auxin receptor F-box protein needed to activate truncated IAA17 by recruiting E3 ubiquitin ligase
pJY1	Flag-Aqp1-DHFR-DD-IRES-EGFP	Inducible expression of Aqp1-DHFR-DD from the minimal CMV promoter
pJY20	Flag-Aqp1-DHFR-IRES-EGFP	Constitutive expression of Aqp1-DHFR-DD from the EF1α promoter
pJY10	Flag-Aqp1-ER-IRES-EGFP	Inducible expression of Aqp1-ER-DD from the minimal CMV promoter

pJY21	Flag-Aqp1-ER-IRES-EGFP	Constitutive expression of Aqp1-ER-DD, from the EF1α promoter
pJY12	Flag-Aqp1-FKBP12-IRES-EGFP	Inducible expression of Aqp1-FKBP12-DD from the minimal CMV promoter
pJY23	Flag-Aqp1-FKBP12-IRES-EGFP	Constitutive expression of Aqp1-FKBP12-DD from the EF1α promoter
pJY24	Flag-FKBP12-Aqp1 -IRES-EGFP	Inducible expression of FKBP12-DD-Aqp1 (i.e. N-terminal tagged) from the minimal CMV promoter
pJY25	Flag-FKBP12-Aqp1 -IRES-EGFP	Constitutive expression of FKBP12-DD-Aqp1 (i.e. N-terminal tagged) from the EF1α promoter
pJY00	Flag-Aqp1-IRES-EGFP	Inducible expression of degron-free Aqp1 from the minimal CMV promoter
pJY23_flag7	Aqp1(flag)-FKBP12-IRES-EGFP	Constitutive expression of Aqp1 with an internal FLAG tag (between Q43 and T44) from the EF1α promoter
pPackaging		Expresses proteins for lentiviral packaging
pVSV-G		Expresses the VSV-G protein for broad lentiviral tropism

Table S2: Oligonucleotide primers for qRT-PCR

Primers/gene	**Sequence**
Aqp1_nFLAG_F	TGGACTACAAGGACGACGAC
Aqp1_nFLAG_R	CACCTTCACGTTGTCCTGGA
Aqp1_cFLAG_F	TCTACGACTTCATCCTGGCC
Aqp1_cFLAG_R	CGTCGTCGTCCTTGTAGTCT
CgACTB_F	CCCCATTGAACACGGCATTG
CgCTB_R	AGGTCTCAAACATGATCTGGGT
HsACTB_F	TTGGCAATGAGCGGTTCC
HsACTB_R	GTTGAAGGTAGTTTCGTGGATG